Journal of Nanophotonics

Nanophotonics.SPIEDigitalLibrary.org

Characterization of polycrystalline silicon-based photonic crystal-suspended membrane for high temperature applications

Chong Pei Ho
Prakash Pitchappa
Piotr Kropelnicki
Jian Wang
Hong Cai
Yuandong Gu
Chengkuo Lee

SPIE.

Characterization of polycrystalline silicon-based photonic crystal-suspended membrane for high temperature applications

Chong Pei Ho,[a,b] Prakash Pitchappa,[a,b] Piotr Kropelnicki,[b,†] Jian Wang,[b] Hong Cai,[b] Yuandong Gu,[b] and Chengkuo Lee[a,*]

[a]National University of Singapore, Department of Electrical and Computer Engineering, Singapore 117576, Singapore

[b]Institute of Microelectronics, Agency for Science, Technology and Research (A*STAR), Singapore 117685, Singapore

Abstract. We present the design and the characterization of a polycrystalline silicon (Si)-based photonic crystal (PhC)-suspended membrane, working in the mid-infrared wavelengths. In order to facilitate transmission measurement, the PhC membrane is released by removing the underneath Si substrate. Around 97% reflection and 3% transmission at 3.58-μm wavelength are measured at room temperature. Characterization is also done at 450°C and it reveals that the peak reflection of the PhC membrane shifts by 75 nm to higher wavelengths. This corresponds to a linear wavelength shift of 0.174 nm/°C and the thermo-optic coefficient is calculated to be $+1.70 \times 10^{-4}$ K^{-1}. By altering the dimension of the PhC air holes, it is also shown that such a thermo-optic effect is compensated. © *2014 Society of Photo-Optical Instrumentation Engineers (SPIE)* [DOI: 10.1117/1.JNP.8.084096]

Keywords: optics; photonic crystal membrane; thermo-optic effect; high temperature applications.

Paper 14027SS received Mar. 7, 2014; revised manuscript received Apr. 27, 2014; accepted for publication Jun. 23, 2014; published online Jul. 15, 2014.

1 Introduction

Two-dimensional (2-D) photonic crystal (PhC) reflectors have been attracting great research interest due to their exceptional optical performance.[1,2] 2-D PhC has been shown to display much lower intrinsic losses,[3–13] and high reflection in PhC can be realized through the use of only a single layer of dielectric. This reduces residual stress with the deposited films especially when working in long wavelengths such as the mid-infrared (MIR) region. In view of these benefits, a 2-D PhC reflector has been proposed to be integrated with optoelectronics devices. One important application of a 2-D PhC reflector is in the realization of a Fabry–Perot interferometer (FPI), which has been used as an optical filter. By arranging two highly reflective mirrors in parallel and separated by a gap distance of $n\lambda/2$, where n is an integer and λ is the desired filtered wavelength, high transmission of only the desired wavelength can be achieved.

Tunability of the output wavelength can be obtained by incorporating microelectromechanical systems technology to change the gap distance.[14] Current methods to form the highly reflective mirror typically employ the use of multilayered structures,[15–18] which require high actuation voltage and the deposition of thicker layers for the FPI to work in the MIR regions for gas sensing. This leads to complicated fabrication. Hence, the use of a 2-D PhC as the reflective mirror is a very viable option to mitigate the difficulties faced in multilayered structures.[19,20] One important application that such FPIs can be used for is in gas sensing, where the identification of gas composition is needed in many industrial processes.[21–24] Methane is an explosive gas and is a

†Current address: Excelitas Technologies, 8 Tractor Road, Singapore 627969, Singapore.

*Address all correspondence to: Chengkuo Lee, E-mail: elelc@nus.edu.sg

primary gas ingredient in mining.[25] In industrial applications such as down-hole oil drilling, detection of methane gas provides information for the drilling process and hence determines the stop point where the drilling is completely exhausted. It is expected that the gas detector will be required to work in a high temperature harsh environment in such an application.

The thermo-optic effect is a well-known phenomenon where the optical property, namely the refractive index, of a material varies with temperature change. In the case of down-hole oil drilling where a high operation temperature is expected, the thermo-optic effect has to be taken into account for design optimization. Numerous works have recently been done to characterize the impact of temperature change on the optical performance of photonic devices.[26–29] Through greater understanding of the thermo-optic effect, efforts are also being made to harness the effect for applications such as optical switches, optical filters, and temperature sensors.[30–39] However, in applications where the thermo-optic effect is undesirable, the temperature effect on the optical performance has to be compensated.[40,41]

In this work, we present the design and the characterization of a polycrystalline Si-based PhC-suspended membrane, working in the MIR wavelengths. In our previous effort, the Si substrate underneath the PhC layer was not removed and this will pose problems when integrating a PhC reflector in FPI.[20] In this work, we demonstrate a free-standing polycrystalline Si-based PhC membrane where the Si substrate is removed. In particular, the high reflection wavelength is desired to be around 3.55 μm, which is the absorption wavelength range of methane gas. Characterization of both the reflection and the transmission is done at room temperature. Experimental measurements show that around 97% reflection and 3% transmission at a 3.58-μm wavelength are obtained for the PhC membrane. In order to show the feasibility of such a PhC membrane in applications such as down-hole oil drilling, characterization is also done up to 450°C. Due to the high temperature, the peak reflection of the PhC membrane shifts by 75 nm to higher wavelengths. This corresponds to a linear wavelength shift of 0.174 nm/°C. In order to ensure that the peak reflection of the PhC membrane remains around 3.55-μm wavelength, we have demonstrated that the thermo-optic effect can be compensated by altering the dimension of the PhC air holes.

2 Design and Simulation of Polycrystalline Si-Based Photonic Crystal Membrane

As the intrinsic absorption wavelength of methane is around 3.55 μm, the output wavelength of the FPI is designed to be at 3.55 μm. This means that the design of the PhC membrane reflector should display high reflection at 3.55 μm as well. The design of the polycrystalline Si-based PhC-suspended membrane is shown in Fig. 1(a). In order to examine the reflection and the transmission characteristics of the PhC membrane, the Si substrate is removed. For high reflection and low transmission at 3.55 μm, the thickness, t, the radius, r, and lattice constant, a, are designed to be 1 μm, 760 nm, and 1.95 μm, respectively, as shown in Fig. 1(b).

Fabrication of the PhC-suspended membrane begins with growing a 1-μm thermal SiO_2 at 1050°C on a bare 8″ Si wafer. The device layer of 1-μm-thick polycrystalline Si is then deposited using low pressure chemical vapor deposition (LPCVD). This is followed by a thermal anneal at

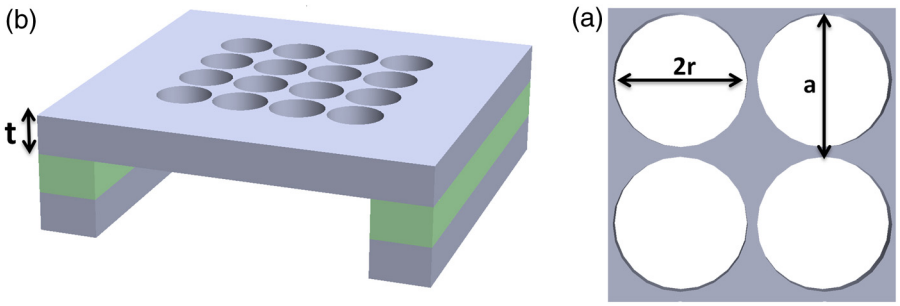

Fig. 1 (a) Schematic of fully released photonic crystal (PhC) membrane with etched air holes. The Si substrate and BOX SiO_2 are removed using deep reactive ion etching and the vapor hydrofluoric acid. (b) Top view of the PhC membrane with the radius of the air holes defined as r, the period as a and the thickness of the polycrystalline Si as t.

1000°C for 30 min to reduce the residual stress within the device layer. The air holes are then patterned using deep-UV lithography and etched using deep reactive ion etching (DRIE). Before proceeding to release the PhC membrane from the Si substrate, the front of the wafer is covered with 1-μm-thick plasma-enhanced chemical vapor deposition (PECVD) SiO_2. The back of the wafer is then patterned using photolithography and DRIE is used to etch the Si substrate. Finally, the whole PhC membrane is released using vapor hydrofluoric acid. The fabricated PhC membrane is shown in Fig. 2. The radius of the air holes and the lattice constant of the PhC structure are observed as 760 nm and 1.95 μm, respectively, with little variation along the PhC membrane.

Simulations of the optical performance of the PhC-suspended membrane are done using finite difference time domain methodology. The permittivity of the polycrystalline Si is set to 12, and periodic boundary conditions are used on the sides of the unit cell.[20] The incidence angle of the input light beam is set to 45 deg, which is consistent with the experimental setup that is used for measurement. The simulated reflection result is overlaid with the measurement results as shown in Fig. 3(a). Generally, the simulated result agrees with the measurement data and both show high reflection around 3.58 μm. A sharp dip in reflection is also found at 3.47 μm, and such a dip in reflection is attributed to the nonzero angle of incidence according to Crozier et al.[43] In this case, the incidence angle is set to 45 deg. In Fig. 3(b), the transmission characteristic of the PhC membrane is examined. A similar spike is also observed in the transmission spectrum at 3.47 μm and this can also be attributed to the incidence angle of 45 deg. In both the simulation and the measurement, low transmission is shown in wavelength regions that exhibit high reflection.

3 Measurement of Polycrystalline Si-Based Photonic Crystal-Suspended Membrane

The Agilent (Santa Clara, California) Cary 620 Fourier transform infrared spectroscopy (FTIR) microscope equipped with a mercury cadmium telluride (MCT) detector is used to measure both reflection and transmission spectra from 2 to 8 μm. Figure 4(a) shows the schematic of the PhC membrane with the incident MIR light. The incidence angle, θ, is set to 45 deg and the incident beam plane angle, φ, is 0 deg. Figure 4(b) shows the measured reflection spectrum normalized against a gold sample, which has around 97% reflection in the MIR region.[44] As r increases, it can be seen that the wavelength of the peak reflection decreases due to the lower refractive index of the PhC membrane. With the radius of the air hole at 760 nm, the peak reflection wavelength is at 3.58 μm, which makes these design parameters suitable for the formation of the highly reflective mirror to be used in the FPI for the detection of methane. The dips that appear in the measured reflection are, as mentioned above, due to the 45-deg angle of incidence of the FTIR microscope used. The inset of Fig. 4(b) indicates the IR image of the PhC membrane at 3.58 μm during measurement. From the diagram, it is conclusive that the peak reflection shown at 3.58-μm wavelength is only due to the PhC-suspended membrane. After the Si substrate is removed, the transmission spectra of the PhC membranes are measured and shown in Fig. 4(c). Again, the measured results are normalized against air and no object is placed along the light path of the source to the MCT detector. Similar to the reflection spectrum, when r is fixed at

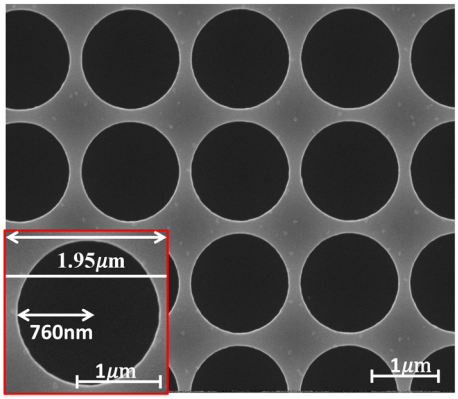

Fig. 2 Scanning electron microscope (SEM) image of the fabricated device with r fixed at 760 nm.

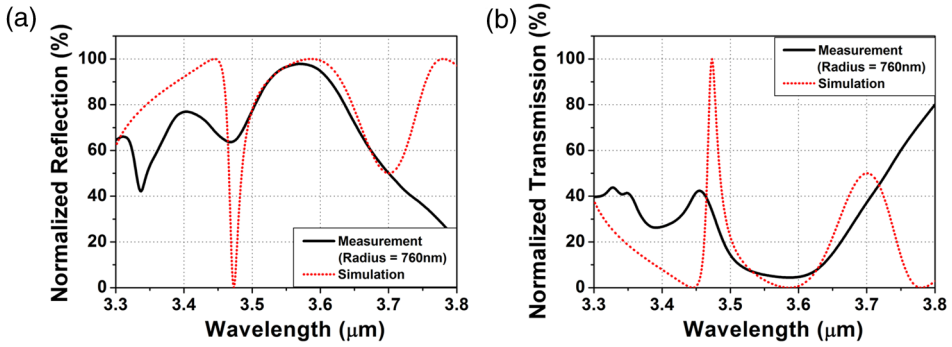

Fig. 3 (a) Simulated reflection (dashed) being overlaid onto the measurement result (solid) showing the high reflection around 3.55-μm wavelength. (b) Simulated transmission (dashed) being overlaid onto the measurement result (solid) showing the low transmission around 3.55-μm wavelength.

760 nm, the transmission drops to the lowest value at around 3.58 μm. As r increases, the wavelengths at which low transmission is measured also display the tendency to shift to lower wavelengths. As low transmission wavelengths in the spectrum show high reflection as well, this indicates that there is low loss within the PhC membrane structure.

4 Effect of Temperature on the Performance of PhC Membrane

The change in peak reflection wavelength of the PhC membrane due to thermo-optic effect of polycrystalline Si is quantified by

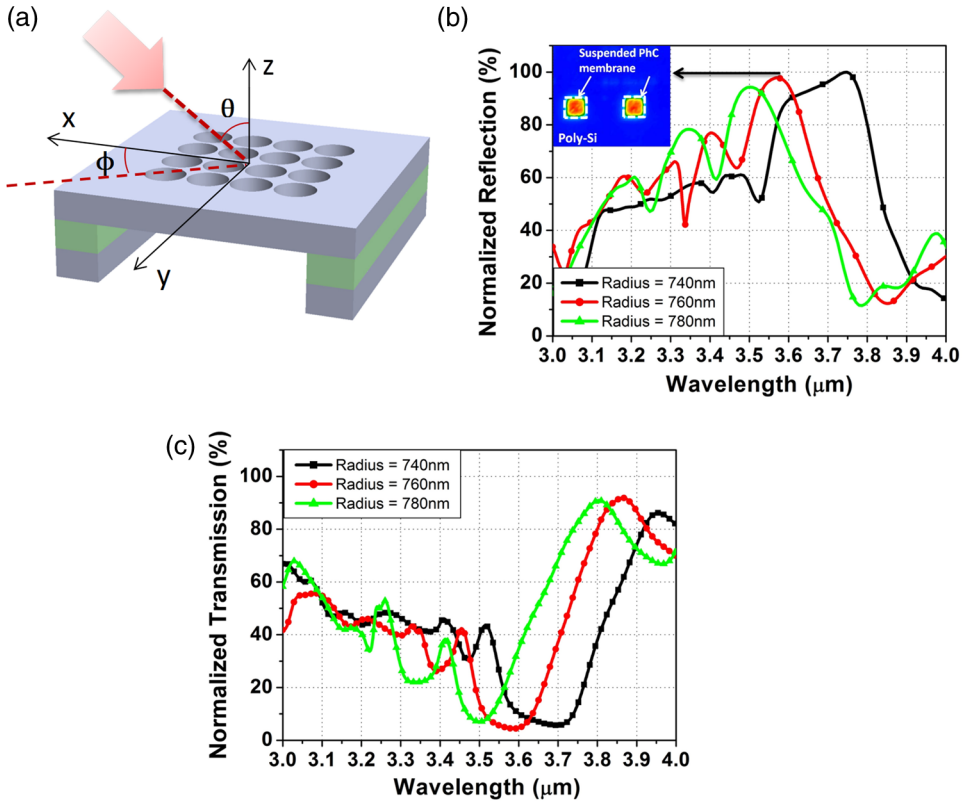

Fig. 4 (a) Schematic of the PhC membrane with the incident mid-infrared light, with the incident angle θ and incident beam plane angle φ. (b) Measured reflection of PhC membranes with different air hole radius, r. The inset is the IR image of the sample taken at 3.58 μm of the sample when r is 760 nm. (c) Measured transmission of PhC membranes with various air hole radii.

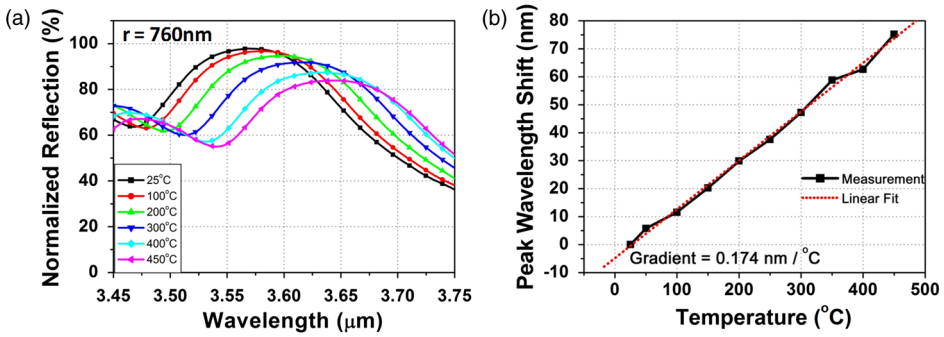

Fig. 5 (a) Measured reflection of PhC membranes at various temperatures up to 450°C. (b) The relationship between the shift in the peak reflection wavelength against temperature and its corresponding linear fit line.

$$\Delta\lambda = \Delta T\left(\frac{\lambda_0}{n_0}\right)\left(\frac{\Delta n}{\Delta T}\right), \tag{1}$$

where n_0 is the refractive index at 25°C, $\Delta n/\Delta T$ is the thermo-optic coefficient, and ΔT is the temperature change. The n_0 is taken to be 3.464 in this work. The PhC-suspended membrane is placed on a heating stage, which is capable of heating up to 450°C. The temperature within the stage is controlled by a temperature controller with a variation of less than ±5%. The measurement results of the PhC membrane with r at 760 nm are shown in Fig. 5(a). At a room temperature of 25°C, the peak reflection is around 3.58 μm which is the intended operating wavelength. As temperature increases, the refractive index of the polycrystalline Si in the PhC-suspended membrane increases. As predicted by Eq. (1), it induces a redshift in the peak reflection. At 450°C, the reflection is located at 3.65 μm and also experiences a drop in maximum intensity. The relationship between the shifts in the peak reflection wavelength is plotted in Fig. 5(b). The shift in the wavelength as temperature increases is 75 nm at 450°C. From the linear fit line of the measurement results, it is measured that the thermo-optic effect induces a shift of 0.174 nm/°C temperature change. Using Eq. (1), the thermo-optic coefficient can be calculated to be $+1.70 \times 10^{-4}$ K^{-1} which is near to the value quoted by other works, where $\Delta n/\Delta T = +1.86 \times 10^{-4}$ K^{-1} (Ref. 42) and $\Delta n/\Delta T = +1.80 \times 10^{-4}$ K^{-1} (Ref. 31).

In order to compensate the thermo-optic effect, a simple methodology is to alter the air hole dimensions when designing the device. Based on the measured data, in order to achieve a maximum reflection at 3.55 μm at 450°C, the PhC membrane should show maximum reflection at a 3.47-μm wavelength at room temperature. This coincides with the performance of the PhC-suspended membrane with an r of 780 nm. The measurements of the devices are shown in Fig. 6. As expected, the reflection displayed by the PhC-suspended membrane with r at 780 nm shows a peak reflection at around 3.56 μm. This shows that the thermo-optic effect which causes the reflection to redshift has been compensated through simple alteration of the dimensions of the air holes. Based on this methodology of optimizing the air hole

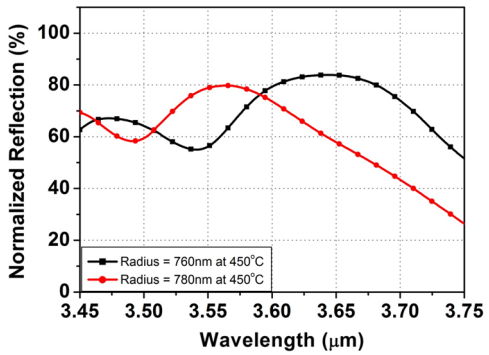

Fig. 6 Measurement of PhC membrane with r at 760 and 780 nm at 450°C.

radius of the PhC-suspended membrane, the desired optical performance can be achieved at various temperatures. This is important for industrial applications such as gas sensing in the down-hole oil drilling process where high temperatures are expected.

5 Conclusion

We have shown the design and characterization of a polycrystalline Si-based PhC-suspended membrane reflector to be used in the MIR wavelengths. As the intended application is for the sensing of hydrocarbons, the design wavelength is fixed at 3.55 μm. The measured reflection and transmission spectra of the PhC-suspended membrane indicate that around 97% reflection and 3% transmission at a 3.58-μm wavelength are obtained at room temperature. Measurements done at 450°C reveal that the thermo-optic effect induces a linear shift of 0.174 nm/°C temperature change. The thermo-optic coefficient is calculated as $+1.70 \times 10^{-4}$ K^{-1}. In order to compensate the redshift of 75 nm induced by the thermo-optic effect, a simple methodology of changing the air hole dimension is feasible. Measured data of the PhC-suspended membrane with an r of 780 nm at 450°C support the fact that such a thermo-optic effect is compensated. Based on this methodology of optimizing the air hole radius, the use of PhC-suspended membrane for applications involving high operating temperatures such as gas sensing in the down-hole oil drilling process can be designed and achieved with the desired optical characteristics.

Acknowledgments

The authors would like to acknowledge the support by SERC Grant Nos. 1021650084 from A*STAR, Singapore, and MOE2012-T2-2-154 (Monolithic Integrated Si/AlN Nanophotonics Platform for Optical NEMS and OEICs) under WBS No. R-263-000-A59-112.

References

1. A. Chadha et al., "Polarization- and angle-dependent characteristics in two dimensional photonic crystal membrane reflectors," *Appl. Phys. Lett.* **103**(21), 211107 (2013).
2. Y. Shuai et al., "Coupled double-layer Fano resonance photonic crystal filters with lattice-displacement," *Appl. Phys. Lett.* **103**(24), 241106 (2013).
3. F. L. Hsiao and Y. T. Ren, "Computational study of slot photonic crystal ring-resonator for refractive index sensing," *Sens. Actuators A: Phys.* **205**, 53–57 (2014).
4. L. Hui et al., "Enhanced focusing properties using surface plasmon multilayer gratings," *IEEE Photonics J.* **4**(1), 57–64 (2012).
5. M. Carras et al., "Room-temperature continuous-wave metal grating distributed feedback quantum cascade lasers," *Appl. Phys. Lett.* **96**(16), 161105 (2010).
6. L. Liyang et al., "Mode-selective hybrid plasmonic Bragg grating reflector," *IEEE Photonics Technol. Lett.* **24**(19), 1765–1767 (2012).
7. Z. Yu et al., "Reflective polarizer based on a stacked double-layer subwavelength metal grating structure fabricated using nanoimprint lithography," *Appl. Phys. Lett.* **77**(7), 927–929 (2000).
8. A. Liu et al., "Polarization-insensitive subwavelength grating reflector based on a semiconductor-insulator-metal structure," *Opt. Express* **20**(14), 14991–15000 (2012).
9. H. Yu et al., "Scanning grating based in-plane movement sensing," *J. Micromech. Microeng.* **20**(8), 085007 (2010).
10. C. Ndiaye et al., "Optimal design for 100% absorption and maximum field enhancement in thin-film multilayers at resonances under total reflection," *Appl. Opt.* **50**(9), C382–C387 (2011).
11. T. M. Jordan, J. C. Partridge, and N. W. Roberts, "Non-polarizing broadband multilayer reflectors in fish," *Nat. Photonics* **6**, 759–763 (2012).
12. T. D. Corrigan et al., "Broadband and mid-infrared absorber based on dielectric-thin metal film multilayers," *Appl. Opt.* **51**(8), 1109–1114 (2012).

13. W. Shen et al., "Narrow band filters in both transmission and reflection with metal/dielectric thin films," *Opt. Commun.* **282**(2), 242–246 (2009).
14. C. C. Chang et al., "Design, fabrication, and characterization of tunable cat's eye retroreflector arrays as optical identification tags," *J. Lightwave Technol. (SCI, EI)* **32**(3), 384–391 (2014).
15. A. J. Keating et al., "Design and Characterization of Fabry–Pérot MEMS-based short-wave infrared microspectrometers," *J. Electron. Mater.* **37**(12), 1811–1820 (2008).
16. J. S. Milne et al., "Widely tunable MEMS-based Fabry Perot filter," *J. Microelectromech. Syst.* **18**(4), 905–913 (2009).
17. T. J. Russin et al., "Fabrication and analysis of a MEMS NIR Fabry Perot interferometer," *J. Microelectromech. Syst.* **21**(1), 181–189 (2012).
18. M. Malak et al., "Cylindrical surfaces enable wavelength-selective extinction and sub-0.2 nm linewidth in 250 μm-Gap Silicon Fabry-Perot cavities," *J. Microelectromech. Syst.* **21**(1), 171–180 (2012).
19. W. Suh et al., "Displacement-sensitive photonic crystal structures based on guided resonance in photonic crystal slabs," *Appl. Phys. Lett.* **82**(13), 1999–2001 (2003).
20. C. P. Ho et al., "Development of polycrystalline silicon based photonic crystal membrane for Mid-Infrared applications," *IEEE J. Sel. Top. Quantum Electron.* **20**(4), 1–7 (2014).
21. X. J. Wu et al., "Application research of hollow-core photonic crystal fibers in methane sensing system," in *2010 8th World Congress on Intelligent Control and Automation (WCICA)*, Jinan, China, Vol. **4**, pp. 811–815 (2010).
22. M. Noro et al., "CO_2/H_2O gas sensor using a tunable Fabry-Perot filter with wide wavelength range," in *IEEE MEMS-03 Kyoto IEEE The Sixteenth Annual Int. Conf. on Micro Electro Mechanical Systems*, Kyoto, Japan, pp. 319–322 (2003).
23. J. Wöllenstein et al., "Miniaturized multi channel infrared optical gas sensor system," *Proc. SPIE* **8066**, 80660Q (2011).
24. J. Mayrwöger et al., "Fabry–Perot-based thin film structure used as IR-emitter of an NDIR gas sensor: ray tracing simulations and measurements," *Proc. SPIE* **8066**, 80660K (2011).
25. Z. J. Yu et al., "Hazard of coal mine gas and its preventive measures," *Adv. Mater. Res.* **724**, 1289–1292 (2013).
26. W. Song et al., "The influence of substrate on SOI photonic crystal thermo-optic devices," *Opt. Express* **21**(4), 4235–4243 (2013).
27. J. V. Malik et al., "Effect of temperature on photonic band gaps in semiconductor-based one-dimensional photonic crystal," *Adv. Opt. Technol.* **2013**, 798087 (2013).
28. C. Markos, K. Vlachos, and G. Kakarantzas, "Bending loss and thermo-optic effect of a hybrid PDMS/silica photonic crystal fiber," *Opt. Express* **18**(23), 24344–24351 (2010).
29. H. G. Teo et al., "Photonic bandgap crystal resonator enhanced laser controlled modulations of optical interconnects for photonic integrated circuits," *Opt. Express* **16**(11), 7842–7848 (2008).
30. W. S. Fegadolli et al., "Reconfigurable silicon thermo-optical ring resonator switch based on Vernier effect control," *Opt. Express* **20**(13), 14722–14733 (2012).
31. D. M. Beggs et al., "Ultracompact and low-power optical switch based on silicon photonic crystals," *Opt. Lett.* **33**(2), 147–149 (2008).
32. D. Hohlfeld, M. Epmeier, and H. Zappe, "A thermally tunable, silicon-based optical filter," *Sens. Actuators A: Phys.* **103**(1), 93–99 (2003).
33. W. Qian et al., "High-sensitivity temperature sensor based on an alcohol-filled photonic crystal fiber loop mirror," *Opt. Lett.* **36**(9), 1548–1550 (2011).
34. H. Lu et al., "Integrated temperature sensor based on an enhanced pyroelectric photonic crystal," *Opt. Express* **21**(14), 16311–16318 (2013).
35. E. A. Camargo, H. Chong, and R. De La Rue, "2D photonic crystal thermo-optic switch based on AlGaAs/GaAs epitaxial structure," *Opt. Express* **12**(4), 588–592 (2004).
36. W. M. Zhu et al., "Micromachined optical well structure for thermo-optic switching," *Appl. Phys. Lett.* **91**(26), 261106 (2007).
37. W. M. Zhu et al., "A micromachined optical double well for thermo-optic switching via resonant tunneling effect," *Appl. Phys. Lett.* **92**(25), 251101 (2008).

38. L. Zhou et al., "Tunable vernier microring optical filters with-type microheaters," *IEEE Photonics J.* **5**(4), 6601211 (2013).
39. J. Tan, R. Soref, and W. Jiang, "Interband scattering in a slow light photonic crystal waveguide under electro-optic tuning," *Opt. Express* **21**(6), 6756–6763 (2013).
40. S. M. Tripathi et al., "Temperature insensitive high-precision refractive-index sensor using two concatenated dual-resonance long-period gratings," *Opt. Lett.* **38**(10), 1666–1668 (2013).
41. Y. Wang et al., "Temperature-insensitive refractive index sensing by use of micro Fabry–Pérot cavity based on simplified hollow-core photonic crystal fiber," *Opt. Lett.* **38**(3), 269–271 (2013).
42. M. W. Pruessner et al., "Thermo-optic tuning and switching in SOI waveguide Fabry-Perot microcavities," *Opt. Express* **15**(12), 7557–7563 (2007).
43. K. B. Crozier et al., "Air-bridged photonic crystal slabs at visible and near-infrared wavelengths," *Phys. Rev. B* **73**(11), 115126 (2006).
44. D. B. Nash, "Mid-infrared reflectance spectra (2.3–22 μm) of sulfur, gold, KBr, MgO, and halon," *Appl. Opt.* **25**(14), 2427–2433 (1986).

Chong Pei Ho received his BEng degree from the Department of Electrical and Computer Engineering at National University of Singapore in 2011. He is currently a research engineer in the same department and also has been enrolled in the NUS PhD program since January 2012. His research interests include applications involving nanophotonics.

Prakash Pitchappa received his BEng degree in electronics and communications from the College of Engineering, Guindy, Anna University, India, in 2008 and his MSc degree from Department of Electrical and Computer Engineering at National University of Singapore (NUS). He enrolled in the NUS PhD program in January 2012, where he is currently a research engineer and is connected to the Institute of Microelectronics (IME), A*STAR. His research interests include the development and of fabrication MEMS-based metamaterials devices.

Piotr Kropelnicki received his diplom ingenieur degree in electrical and electronics engineering in 2007 from Universität Duisburg-Essen, Germany, with a major in microelectronics. He finished his PhD degree in microelectronics at Fraunhofer Institute for Microelectronic Circuit and Systems in 2010. He is currently a principal investigator, leading a team in the SAM-Sensors and Actuators Microsystems Program at the Institute of Microelectronics. He is responsible for the development of several sensors operating in harsh environments, such as pressure, gas detection, optical, viscosity, and temperature sensors.

Jian Wang received his PhD degree from the Department of Electrical and Computer Engineering at National University of Singapore. He is currently in the Department of MEMS of the Institute of Microelectronics, Agency for Science, Technology and Research (A*STAR), Singapore. His research interest is in MEMS integration processes.

Hong Cai received her PhD degree from Nanyang Technological University, Singapore, in 2009. She is currently a research scientist with the Institute of Microelectronics, Agency for Science, Technology and Research (A*STAR), Singapore. Her research interests include optical and photonics MEMS/NEMS and nanosensors development.

Yandong Gu received his PhD and MEE from the Department of Pharmaceutics and Electrical Engineering at the University of Minnesota in 2002. He is the technical director of the Institute of Microelectronics, Agency for Science, Technology and Research (A*STAR). His research interests are optical-based chemical sensing, AlN-based sensors and actuators, and miniaturized medical instrumentation.

Chengkuo Lee received his PhD in precision engineering from the University of Tokyo, Japan, in 1996. He is currently an associate professor in the Department of Electrical and Computer Engineering, National University of Singapore. He has published more than 200 conference papers and extended abstracts, 160 peer-reviewed journal articles, and nine U.S. patents in the MEMS, NEMS, metamaterials, nanophotonics, and nanotechnology fields.